

Cooling of Hybrid Neutron Stars and Hypothetical Self-bound Objects with Superconducting Quark Cores

D. Blaschke^{1,2}, H. Grigorian^{1,3}, and D.N. Voskresensky⁴

¹ Fachbereich Physik, Universität Rostock, Universitätsplatz 1, D-18051 Rostock, Germany
email: blaschke@darss.mpg.uni-rostock.de

² European Centre for Theoretical Studies ECT*, Villa Tambosi, Strada delle Tabarelle 286, 38050 Villazzano (Trento), Italy

³ Department of Physics, Yerevan State University, Alex Manoogian Str. 1, 375025 Yerevan, Armenia
email: hovik@darss.mpg.uni-rostock.de

⁴ Moscow Institute for Physics and Engineering, Kashirskoe shosse 31, 115409 Moscow, Russia
Gesellschaft für Schwerionenforschung GSI, Planckstrasse 1, D-64291 Darmstadt, Germany
email: D.Voskresensky@gsi.de

Received 14 September 2000 / Accepted 02 January 2001

Abstract. We study the consequences of superconducting quark cores (with color-flavor-locked phase as representative example) for evolution of temperature profiles and the cooling curves in quark-hadron hybrid stars and in hypothetical self-bounded objects having no a hadron shell (quark core neutron stars). The quark gaps are varied from 0 to $\Delta_q = 50$ MeV. For hybrid stars we find time scales of $1 \div 5$, $5 \div 10$ and $50 \div 100$ years for the formation of a quasistationary temperature distribution in the cases $\Delta_q = 0$, 0.1 MeV and $\gtrsim 1$ MeV, respectively. These time scales are governed by the heat transport within quark cores for large diquark gaps ($\Delta \gtrsim 1$ MeV) and within the hadron shell for small diquark gaps ($\Delta \lesssim 0.1$ MeV). For quark core neutron stars we find a time scale $\simeq 300$ years for the formation of a quasistationary temperature distribution in the case $\Delta \gtrsim 10$ MeV and a very short one for $\Delta \lesssim 1$ MeV. If hot young compact objects will be observed they can be interpreted as manifestation of large gap color superconductivity. Depending on the size of the pairing gaps, the compact star takes different paths in the $\lg(T_s)$ vs. $\lg(t)$ diagram where T_s is the surface temperature. Compared to the corresponding hadronic model which well fits existing data the model for the hybrid neutron star (with a large diquark gap) shows too fast cooling. The same conclusion can be drawn for the corresponding self-bound objects.

Key words. dense matter – stars: interiors – stars: evolution – stars: neutron

1. Introduction

The interiors of compact stars are considered as systems where high-density phases of strongly interacting matter do occur in nature, see Glendenning (1996) and Weber (1999) for recent textbooks. The consequences of different phase transition scenarios for the cooling behaviour of compact stars have been reviewed recently in comparison with existing X-ray data, see Page (1992), Schaab et al. (1997).

A completely new situation might arise if the scenarios suggested for (color) superconductivity (Alford et al. 1998, Rapp et al. 1998) with large diquark pairing gaps ($\Delta_q \sim 50 \div 100$ MeV) in quark matter are applicable to neutron star interiors. Various phases are possible. The two-flavor (2SC) or the three-flavor (3SC) superconducting phases allow for unpaired quarks

of one color whereas in the color-flavor locking (CFL) phase all the quarks are paired.

Estimates of the cooling evolution have been performed (Blaschke et al. 2000) for a self-bound isothermal quark core neutron star (QCNS) which has a crust but no hadron shell, and for a quark star (QS) which has neither crust nor hadron shell. It has been shown there in the case of the 2SC (3SC) phase of QCNS that the consequences of the occurrence of gaps for the cooling curves are similar to the case of usual hadronic neutron stars (enhanced cooling). However, for the CFL case it has been shown that the cooling is extremely fast since the drop in the specific heat of superconducting quark matter dominates over the reduction of the neutrino emissivity. As has been pointed out there, the abnormal rate of the temperature drop is the consequence of the approximation of homogeneous temperature profiles the applicability of which should be limited by the heat transport effects. Page et

al. (2000) estimated the cooling of hybrid neutron stars (HNS) where heat transport effects within the superconducting quark core have been disregarded. Neutrino mean free path in color superconducting quark matter have been discussed in (Carter & Reddy 2000) where a short period of cooling delay at the onset of color superconductivity for a QS has been conjectured in accordance with the estimates of (Blaschke et al. 2000) in the CFL case for small gaps.

In the present paper we want to consider a more detailed scenario for the thermal evolution of HNS and QCNS which includes the heat transport in both the quark and the hadronic matter. We will demonstrate how long it takes for the HNS and for the QCNS to establish a quasistationary temperature profile and then we consider the influence of both the diquark pairing gaps and the hadronic gaps on the evolution of the surface temperature.

2. Processes in HNS and QCNS

2.1. Processes in quark matter

2.1.1. Emissivity

A detailed discussion of the neutrino emissivity of quark matter without the possibility of color superconductivity has been given first by Iwamoto (1982). In his work the quark direct Urca (QDU) reactions $d \rightarrow ue\bar{\nu}$ and $ue \rightarrow d\nu$ have been suggested as the most efficient processes. Their emissivities have been obtained as ¹

$$\epsilon_{\nu}^{\text{QDU}} \simeq 9.4 \times 10^{26} \alpha_s u Y_e^{1/3} \zeta_{\text{QDU}} T_9^6 \text{ erg cm}^{-3} \text{ s}^{-1}, \quad (1)$$

where at a compression $u = n/n_0 \simeq 2$ the strong coupling constant is $\alpha_s \approx 1$ and decreases logarithmically at still higher densities. The nuclear saturation density is $n_0 = 0.17 \text{ fm}^{-3}$, $Y_e = n_e/n$ is the electron fraction, and T_9 is the temperature in units of 10^9 K . If for somewhat larger density the electron fraction was too small ($Y_e < Y_{ec} \simeq 10^{-8}$), then all the QDU processes would be completely switched off (Duncan et al. 1983) and the neutrino emission would be governed by two-quark reactions like the quark modified Urca (QMU) and the quark bremsstrahlung (QB) processes $dq \rightarrow uqe\bar{\nu}$ and $q_1 q_2 \rightarrow q_1 q_2 \nu \bar{\nu}$, respectively. The emissivities of the QMU and QB processes have been estimated as (Iwamoto 1982)

$$\epsilon_{\nu}^{\text{QMU}} \sim \epsilon_{\nu}^{\text{QB}} \simeq 9.0 \times 10^{19} \zeta_{\text{QMU}} T_9^8 \text{ erg cm}^{-3} \text{ s}^{-1}. \quad (2)$$

Due to the pairing, the emissivities of QDU processes are suppressed by a factor $\zeta_{\text{QDU}} \sim \exp(-\Delta_q/T)$ and the emissivities of QMU and QB processes are suppressed by a factor $\zeta_{\text{QMU}} \sim \exp(-2\Delta_q/T)$ for $T < T_{\text{crit},q} \simeq 0.4 \Delta_q$ whereas for $T > T_{\text{crit},q}$ these factors are equal to unity. The modification of $T_{\text{crit},q}(\Delta_q)$ relative to the standard BCS formula is due to the formation of correlations as, e.g., instanton- anti-instanton

¹ Please notice that the numerical factors in all the estimates below depend essentially on rather unknown factors and thereby can be still varied.

molecules (Rapp et al. 2000). For the temperature dependence of the gap below $T_{\text{crit},q}$ we use the interpolation formula $\Delta(T) = \Delta(0)\sqrt{1 - T/T_{\text{crit},q}}$, with $\Delta(0)$ being the gap at zero temperature.

The contribution of the reaction $ee \rightarrow eev\bar{\nu}$ is very small (Kaminker & Haensel 1999)

$$\epsilon_{\nu}^{ee} = 2.8 \times 10^{12} Y_e^{1/3} u^{1/3} T_9^8 \text{ erg cm}^{-3} \text{ s}^{-1}, \quad (3)$$

but it can become important when quark processes are blocked out for large values of Δ_q/T in superconducting quark matter.

2.1.2. Specific heat

For the quark specific heat we use an expression (Iwamoto 1982)

$$c_q \simeq 10^{21} u^{2/3} \zeta_S T_9 \text{ erg cm}^{-3} \text{ K}^{-1}, \quad (4)$$

where $\zeta_S \simeq 3.1 (T_{\text{crit},q}/T)^{5/2} \exp(-\Delta_q/T)$. Besides, one should add the gluon-photon contribution (Blaschke et al. 2000)

$$c_{g-\gamma} = 3.0 \times 10^{13} N_{g-\gamma} T_9^3 \text{ erg cm}^{-3} \text{ K}^{-1}, \quad (5)$$

where $N_{g-\gamma}$ is the number of available massless gluon-photon states (which are present even in the color superconducting phase), as well as the electron one,

$$c_e = 5.7 \times 10^{19} Y_e^{2/3} u^{2/3} T_9 \text{ erg cm}^{-3} \text{ K}^{-1}. \quad (6)$$

2.1.3. Heat conductivity

The heat conductivity of the matter is the sum of partial contributions (Flowers & Itoh 1981)

$$\kappa = \sum_i \kappa_i, \quad \frac{1}{\kappa_i} = \sum_j \frac{1}{\kappa_{ij}}, \quad (7)$$

where i, j denote the components (particle species). For quark matter κ is the sum of the partial conductivities of the electron, quark and gluon components (Haensel & Jerzak 1989, Baiko & Haensel 1999)

$$\kappa = \kappa_e + \kappa_q + \kappa_g, \quad (8)$$

where $\kappa_e \simeq \kappa_{ee}$ is determined by electron-electron scattering processes since in superconducting quark matter the partial contribution $1/\kappa_{eq}$ (as well as $1/\kappa_{gq}$) is additionally suppressed by a ζ_{QDU} factor, as for the scattering on impurities in metallic superconductors. For κ_{ee} we have

$$\kappa_{ee} = 5.5 \times 10^{23} u Y_e T_9^{-1} \text{ erg s}^{-1} \text{ cm}^{-1} \text{ K}^{-1}, \quad (9)$$

and

$$\begin{aligned} \kappa_q &\simeq \kappa_{qq} \\ &\simeq 1.1 \times 10^{23} \sqrt{\frac{4\pi}{\alpha_s}} u \zeta_{\text{QDU}} T_9^{-1} \text{ erg s}^{-1} \text{ cm}^{-1} \text{ K}^{-1}, \end{aligned} \quad (10)$$

where we have accounted for the suppression factor. The contribution of massless gluons we estimate as

$$\begin{aligned} \kappa_g &\simeq \kappa_{gg} \\ &\simeq 6.0 \times 10^{17} T_9^2 \text{ erg s}^{-1} \text{ cm}^{-1} \text{ K}^{-1}. \end{aligned} \quad (11)$$

2.2. Processes in hadronic matter

2.2.1. Emissivity

DU processes $n \rightarrow pe\bar{\nu}$, $pe \rightarrow n\nu$ can occur when the proton fraction exceeds 11% (Lattimer et al. 1991). It does not occur for the equation of state we use but there are examples for the opposite case (Page et al. 2000). This is another difference of our present work to the recent one of Page et al. (2000).

Next, we take into account the modified Urca (MU) processes $nn \rightarrow npe\bar{\nu}$, $np \rightarrow ppe\bar{\nu}$, and the reverse processes. The final emissivity is given by (Friman & Maxwell 1979, Yakovlev et al. 1999)

$$\epsilon_\nu^{\text{nMU}} = 8.6 \times 10^{21} m_{\text{nMU}}^{*4} (Y_e u)^{1/3} \zeta_{\text{nMU}} T_9^8 \text{erg cm}^{-3} \text{s}^{-1} \quad (12)$$

$$\epsilon_\nu^{\text{pMU}} = 8.5 \times 10^{21} m_{\text{pMU}}^{*4} (Y_e u)^{1/3} \zeta_{\text{pMU}} T_9^8 \text{erg cm}^{-3} \text{s}^{-1} \quad (13)$$

Here $m_i^* = \sqrt{m_{\text{rel},i}^{*2} + p_{\text{F},i}^2}$ is the non-relativistic quasi-particle effective mass related to the in-medium one-particle energies from a given relativistic mean field model for $i = n, p$. We have introduced the abbreviations $m_{\text{nMU}}^{*4} = (m_n^*/m_n)^3 (m_p^*/m_p)$ and $m_{\text{pMU}}^{*4} = (m_p^*/m_p)^3 (m_n^*/m_n)$. The suppression factors are $\zeta_{\text{nMU}} = \zeta_n \zeta_p \simeq \exp\{-[\Delta_n(T) + \Delta_p(T)]/T\}$, $\zeta_{\text{pMU}} \simeq \zeta_p^2$, and should be replaced by unity for $T > T_{\text{crit},i}$ when for given species i the corresponding gap vanishes. For neutron and proton S -wave pairing, $\Delta_i(0) = 1.76 T_{\text{crit},i}$ and for P -wave pairing of neutrons $\Delta_n(0) = 1.19 T_{\text{crit},n}$. To be conservative we have used in (12) the free one-pion exchange estimate of the NN interaction amplitude. Restricting ourselves to a qualitative analysis we use here simplified exponential suppression factors ζ_i . In a more detailed analysis these ζ_i -factors have prefactors with rather strong temperature dependences Yakovlev et al. 1999. At temperatures $T \sim T_c$ their inclusion only slightly affects the resulting cooling curves. For $T \ll T_c$ the MU process gives in any case a negligible contribution to the total emissivity and thereby corresponding modifications can again be omitted. Also for the sake of simplicity the general possibility of a ${}^3\text{P}_2(|m_J| = 2)$ pairing which may result in a power-law behaviour of the specific heat and the emissivity of the MU process Voskresensky & Senatorov 1987, Yakovlev et al. 1999 is disregarded since mechanisms of this type of pairing are up to now not elaborated. Even more essential modifications of the MU rates may presumably come from in-medium effects which could result in extra prefactors of $10^2 \div 10^3$ already at $T \sim T_c$.

In order to estimate the role of the in-medium effects in the NN interaction for the HNS cooling we have also performed calculations for the so-called medium modified Urca (MMU) process (Voskresensky & Senatorov 1986, Migdal et al. 1990) by multiplying the rates (12) by the appropriate prefactor

$$\epsilon_\nu^{\text{MMU}}/\epsilon_\nu^{\text{MU}} \simeq 10^3 [\Gamma^6(g')/\tilde{\omega}^8(k \simeq p_F)] u^{10/3}, \quad (14)$$

where the value $\Gamma(g') \simeq 1/[1 + 1.4 u^{1/3}]$ is due to the dressing of πNN vertices and $\tilde{\omega} \leq m_\pi$ is the effective pion

gap which we took as function of density from Fig. 2 of (Schaab et al. 1997).

For $T < T_{\text{crit}}$ the most important contribution comes from the neutron (Flowers et al. 1976, Voskresensky & Senatorov 1987, Yakovlev et al. 1999) and the proton (Voskresensky & Senatorov 1987) pair breaking and formation processes. Their emissivities we take from Ref. (Schaab et al. 1997) which is applicable for both the cases of S - and P -wave nucleon pairing

$$\epsilon_\nu^{\text{NPBF}} = 6.6 \times 10^{28} (m_n^*/m_n) (\Delta_n(T)/\text{MeV})^7 u^{1/3} \times \xi I(\Delta_n(T)/T) \text{erg cm}^{-3} \text{s}^{-1}, \quad (15)$$

$$\epsilon_\nu^{\text{PPBF}} = 0.8 \times 10^{28} (m_p^*/m_p) (\Delta_p(T)/\text{MeV})^7 u^{2/3} \times I(\Delta_p(T)/T) \text{erg cm}^{-3} \text{s}^{-1}, \quad (16)$$

where

$$I(\Delta_i(T)/T) \simeq 0.89 \sqrt{T/\Delta_i(T)} \exp[-2\Delta_i(T)/T], \quad (17)$$

$\xi \simeq 0.5$ for 1S_0 pairing and $\xi \simeq 1$ for 3P_2 pairing. A significant contribution of the proton channel is due to the NN correlation effect taken into account in (Voskresensky & Senatorov 1987).

2.2.2. Specific heat

For the nucleons ($i = n, p$), the specific heat is (Maxwell 1979)

$$c_i = 1.6 \times 10^{20} (m_i^*/m_i) u^{1/3} \zeta_{\text{MMU}} T_9 \text{erg cm}^{-3} \text{K}^{-1}. \quad (18)$$

The specific heat for the electrons is determined by (6) and that for the photons for $T > T_{\text{cp}}$ is given by (5) with the corresponding number of polarizations $N_\gamma = 2$.

2.2.3. Heat conductivity

The total conductivity is

$$\kappa \simeq \kappa_n + \kappa_e, \quad \frac{1}{\kappa_n} = \frac{1}{\kappa_{nn}} + \frac{1}{\kappa_{np}}, \quad (19)$$

where the partial contributions are (Flowers & Itoh 1981, Baiko & Haensel 1999)

$$\kappa_{nn} = 8.3 \times 10^{22} \left(\frac{m_n}{m_n^*}\right)^4 \frac{z_n^3 \zeta_n}{S_{kn} T_9} \text{erg s}^{-1} \text{cm}^{-1} \text{K}^{-1}, \quad (20)$$

$$S_{kn} = 0.38 z_n^{-7/2} + 3.7 z_n^{2/5}, \quad (21)$$

$$\kappa_{np} = 8.9 \times 10^{16} \left(\frac{m_n}{m_n^*}\right)^2 \frac{z_n^2 \zeta_p T_9}{z_p^3 S_{kp}} \text{erg s}^{-1} \text{cm}^{-1} \text{K}^{-1}, \quad (22)$$

$$S_{kp} = 1.83 z_n^{-2} + 1.43 z_n^2 (0.4 + z_n^8)^{-1}. \quad (23)$$

Here we have introduced the appropriate suppression factors ζ_i which act in the presence of gaps for superfluid hadronic matter and we have used the abbreviation $z_i = (n_i/(4n_0))^{1/3}$. The heat conductivity of electrons is given by Eq. (9).

2.3. Processes in the mixed phase

In some density interval $n_H < n < n_Q$ we have a mixed phase in the HNS case. Although our treatment of the contribution of the mixed phase to the equation of state is rather poor, for the discussion of the neutrino processes we assume the mixed phase to be constructed as a lattice (for $T < T_{\text{melt}}$) of color superconducting quark droplets embedded in the nucleonic Fermi sea (superfluid for $T < T_{\text{crit},i}; i = n, p$) at densities near the lower boundary density n_H which is reorganized as a lattice of nucleon droplets in the quark Fermi sea near the upper boundary density n_Q . We suppose that the mixed phase contributes to the neutrino reactions and to the heat transport as two homogeneous phases weighted according to their partial volumina and thus suppress reactions on the impurities which could be as efficient as one-nucleon/quark processes in the liquid phase (Reddy et al. 2000). Thus we assume $T < T_{\text{melt}}$ in our case.

2.4. Crust and surface

In order to avoid a complicated analysis of the processes in the crust we use an interpolated relation between the surface and the crust temperatures (see Shapiro & Teukolsky 1983) $T_s = (10 T_m)^{2/3}$, where temperatures are given in K, the so-called Tsuruta law Tsuruta 1979. More elaborated and complicated dependences of T_s on T_m and the parameters of the crust can be found in (Gudmundsson et al. 1982, Gudmundsson et al. 1982, Van Riper 1988, Potekhin et al. 1997). As we have estimated, their inclusion does not affect qualitatively the conclusions of this work. The mantle temperature $T_m = T(r_m)$ we take at the distance r_m from the center where the density is equal to the critical one for the transition to the mixed (Aen) phase. This is correct for time scales exceeding those determined by the heat conductivity of the crust estimated as $\lesssim 10$ yr for hadronic stars and $\lesssim 1$ yr for strange stars (see Pizzochero 1991, Lattimer et al. 1991). Since the crust is rather thin and has a much smaller heat content than the bulk of the star its contribution to the cooling delay for time intervals shorter than the ones given above is negligible. Due to these reasons and for the sake of simplicity we disregard these effects in further considerations.

We also add the photon contribution to the emissivity at the surface

$$\epsilon_\gamma \simeq 2 \times 10^{18} \left(\frac{R}{10 \text{ km}} \right)^{-1} T_{s7}^4 \text{ erg cm}^{-3} \text{ sec}^{-1}, \quad (24)$$

where T_{s7} is the surface temperature in units of 10^7 K, using it as the boundary condition in our transport code. Thus simplifying we assume that the outer crust and the photosphere are thin enough to approximate $r_m \simeq R$, where R is the star radius. Then, the luminosity at r_m corresponds to the surface luminosity of the photons from the star $l(r_m) = L_\gamma(T_s)$.

3. Evolution of inhomogeneous emissivity profiles

3.1. Equation of state and gaps

The equation of state is described according to the model (Chubarian et al. 2000) incorporating three possible phases (depending on the star mass, the value of the bag constant B and other parameters as the mass of the strange quark, the compressibility of hadron matter etc.). These phases are hadronic matter, quark-hadron mixed phase and pure quark matter. As a representative example we consider below a star with a mass of $1.4 M_\odot$ for the neutron star consisting of pure hadronic matter (radius $\simeq 13$ km), for the HNS (radius $\simeq 10$ km) and for the self-bound QCNS (radius $\simeq 9$ km). The typical electron fraction is $Y_e \simeq 0.04$ for the hadronic star which does not allow for the occurrence of direct Urca processes.

For the HNS the electron fraction is $Y_e \simeq 0.03$ for $n = n_H$, where n_H corresponds to the critical density when first seeds of quark phase appear; $Y_e \simeq 8.5 \times 10^{-5}$ for $n = n_Q$ when hadron seeds disappear, i.e. at the boundary of the quark core, and $Y_e \simeq 2 \times 10^{-5}$ for $n = n_c$, i.e. for the baryon density in the star center.

The radius corresponding to $n = n_H$ is $r_H = 8$ km and that corresponding to $n = n_Q$ is $r_Q = 6.5$ km. We take the same dependences $\Delta_i(n)$ for $i = n, p$ as in Fig. 6 of (Schaab et al. 1997). As an alternative example we also consider the model with suppressed gaps to estimate the effect of possible uncertainties. In the mixed phase we take $\Delta_i = \Delta_i(n_H)$ for the hadron sub-system and $\Delta = \Delta_q$ for the quark one, and in the quark phase we for simplicity take $\Delta_q = \text{const}$.

For QCNS besides the case when Y_e is determined from our calculation we consider also $Y_e = 0$ as an extreme example of the case $Y_e < Y_{ec}$, in order to understand its possible consequences. Then direct Urca does not occur also in the quark phase.

3.2. Cooling

Due to the inhomogeneous distribution of matter inside the star and finite heat conductivity the temperature profile $T(r, t)$ during the cooling process can differ from the isothermal equilibrium one for which the temperature on the inner crust boundary (T_m) and the central one (T_c) are connected by the relation $T_m = T_c \exp[\Phi(0) - \Phi(R)]$, where $\Phi(0) - \Phi(R)$ is the difference of the gravitational potentials in the center and at the surface of the star, respectively.

The flux of energy $l(r)$ per unit time through a spherical slice at the distance r from the center is proportional to the gradient of the temperature on both sides of the spherical slice,

$$l(r) = -4\pi r^2 \kappa(r) \frac{\partial(Te^\Phi)}{\partial r} e^{-\Phi} \sqrt{1 - \frac{2M}{r}}, \quad (25)$$

the factor $e^{-\Phi} \sqrt{1 - \frac{2M}{r}}$ corresponds to the relativistic correction of the time scale and the unit of thickness. The

equations for energy balance and thermal energy transport are (Weber 1999)

$$\frac{\partial}{\partial A} (le^{2\Phi}) = -\frac{1}{n} \left(\epsilon_\nu e^{2\Phi} + c_V \frac{\partial}{\partial t} (Te^\Phi) \right), \quad (26)$$

$$\frac{\partial}{\partial A} (Te^{2\Phi}) = -\frac{1}{\kappa} \frac{le^\Phi}{16\pi^2 r^4 n}, \quad (27)$$

where $n = n(r)$ is the baryon number density, $A = A(r)$ is the total baryon number in the sphere with radius r and

$$\frac{\partial r}{\partial A} = \frac{1}{4\pi r^2 n} \sqrt{1 - \frac{2M}{r}}. \quad (28)$$

The total neutrino emissivity ϵ_ν and the total specific heat c_V are given as the sum of the corresponding partial contributions defined in the previous Section for a composition $n_i(r)$ of constituents i of the matter under the conditions of the actual temperature profile $T(r, t)$. The accumulated mass $M = M(r)$ and the gravitational potential $\Phi = \Phi(r)$ can be determined by

$$\frac{\partial M}{\partial A} = \frac{\varepsilon}{n} \sqrt{1 - \frac{2M}{r}}, \quad (29)$$

$$\frac{\partial \Phi}{\partial A} = \frac{4\pi r^3 p + m}{4\pi r^2 n} \frac{1}{\sqrt{1 - \frac{2M}{r}}}, \quad (30)$$

where $\varepsilon = \varepsilon(r)$ is the energy density profile and the pressure profile $p = p(r)$ is defined by the condition of hydrodynamical equilibrium

$$\frac{\partial p}{\partial A} = -(p + \varepsilon) \frac{\partial \Phi}{\partial A}. \quad (31)$$

The boundary conditions for the solution of (26) and (27) read $l(r=0) = l(A=0) = 0$ and $T(A(r_m) = A, t) = T(r_m = R, t) = T_m(t)$, respectively.

In our examples we choose the initial temperature to be 1 MeV. This is a typical value for the temperature T_{opacity} at which the star becomes transparent for neutrinos. Simplifying we disregard the neutrino influence on transport. These effects dominate for $t \lesssim 1 \div 100$ min, when the star cools down to $T \leq T_{\text{opacity}}$ and become unimportant for later times.

4. Temperature evolution of HNS

4.1. Temperature profiles $T(r, t)$

With the above inputs we have solved the evolution equation for the temperature profile. In order to demonstrate the influence of the size of the diquark and nucleon pairing gaps on the evolution of the temperature profile we have performed solutions with different values of the quark and nucleon gaps. The representative examples are shown in Fig. 1. Nucleon gaps are taken the same as in Fig. 6 of (Schaab et al. 1997). The quark gaps larger than 1 MeV show the same typical behaviour as for the gap $\Delta_q = 50$ MeV. The gaps much smaller than 1 MeV exhibit the typical small gap behaviour as for $\Delta_q = 0.1$ MeV in our example.

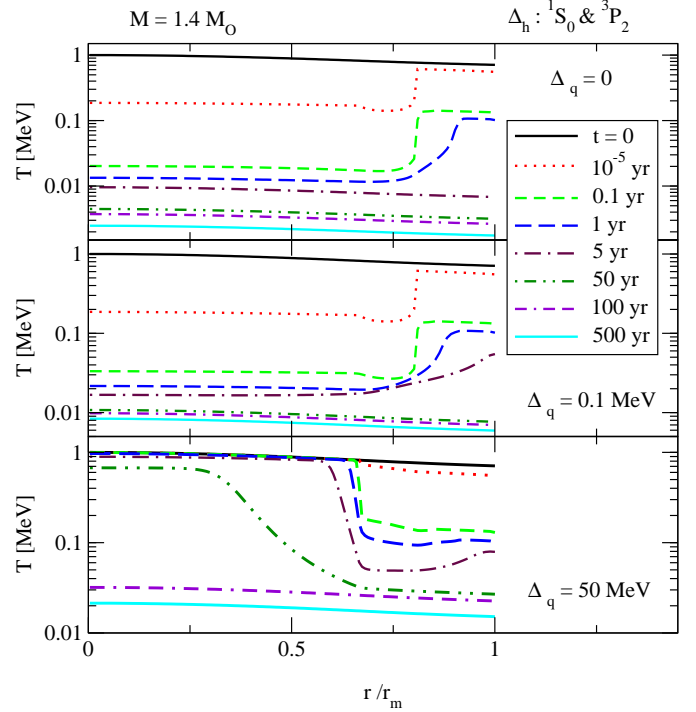


Fig. 1. Early evolution of temperature profiles for a HNS of $M = 1.4M_\odot$ with large (lower panel), small (middle) and vanishing (upper panel) diquark pairing gaps.

For large quark gaps, the hadron phase cools down on the time scale $t \simeq 0.1 \div 5$ yr due to the heat transport to the star surface whereas the quark core keeps the heat during this time. Therefore, if an independent measurement of the core temperature was possible, e.g. by neutrinos, then a core temperature stall during first several years of cooling evolution would be a case for quark core superconductivity with large pairing gaps. Then the quark core begins to cool down slowly from its mixed phase boundary, the cold from hadrons via mixed phase spreads to the center, demonstrating that the direct neutrino radiations during all the time are inefficient within the quark core. The homogeneous temperature profile is recovered at typical times of $t \simeq 50 \div 100$ yr.

For $\Delta_q = 0.1$ MeV the QDU processes and the heat conductivity within the quark core are quite efficient. Therefore at very small times ($t \ll 10^{-5}$ yr) the temperature profile within the quark core is a homogeneous one whereas during the next $5 \div 10$ yr the hadron shell is cooled down from the both sides, the mixed phase boundary at $n(r_H) = n_H$ and the star surface. Thus, for $\Delta_q \ll 1$ MeV the interior evolution of the temperature has an influence on the surface temperature from the very early times. Actually the shortest time scale which determines the slowing of the heat transport within the crust is in this case $t \sim 1$ yr. Thus at much smaller times one has $T_s(t) \simeq T_s(0)$ with a drop of $T(r, t)$ in the vicinity of $r/r_m = 1$. Due to the relatively small heat content of the crust this peculiar effect is disregarded here.

Qualitatively the same behaviour is illustrated for normal quark matter with the only difference that quantitatively the quark processes are more efficient at $\Delta_q = 0$ and the cold thereby traverses the hadron phase more rapidly, at typical times $t \simeq 1 \div 5$ yr.

4.2. Evolution of the surface temperature

A detailed comparison of the cooling evolution ($\lg T_s$ vs. $\lg t$) of HNS for different values of quark and hadron gaps is given in Fig. 2. We have found that the curves for $\Delta_q \gtrsim 1$ MeV are very close to each other demonstrating typical large gap behaviour. As representative example we again take $\Delta_q = 50$ MeV. The behaviour of the cooling curve for $t \leq 50 \div 100$ yr is in straight correspondence with the heat transport processes discussed above. The subsequent time evolution is governed by the processes in the hadronic shell and by a delayed transport within the quark core with a dramatically suppressed neutrino emissivity from the color superconducting region. In order to demonstrate this feature we have performed a calculation with the nucleon gaps ($\Delta_i(n)$, $i = n, p$) being artificially suppressed by a factor 0.2. Then up to $\lg(t[\text{yr}]) \lesssim 4$ the behaviour of the cooling curve is analogous to the one we would have obtained for pure hadronic matter. The curves labelled "MMU" are calculated with the rates of modified Urca processes of Eq. (12) multiplied by the factor (14), i.e. with inclusion of appropriate medium modifications in the NN interaction. As can be seen from Fig. 2, these effects have an influence on the cooling evolution only for $\lg(t[\text{yr}]) \lesssim 2$ since our specific model equation of state does not allow for large nucleon densities in the hadron phase for the $M = 1.4 M_\odot$ neutron star under discussion. The effect would be more pronounced for larger star masses, a softer equation of state for hadron matter and smaller values of the gaps in the hadronic phase.

The unique asymptotic behaviour at $\lg(t[\text{yr}]) \geq 5$ for all the curves corresponding to finite values of the quark and nucleon gaps is due to a competition between normal electron contribution to the specific heat and the photon emissivity from the surface since small exponentials switch off all the processes related to paired particles. This tail is very sensitive to the interpolation law $T_s = f(T_m)$ used to simplify the consideration of the crust. The curves coincide at large times due to the uniquely chosen relation $T_s \propto T_m^{2/3}$.

The curves for $\Delta_q = 0.1$ MeV demonstrate an intermediate cooling behaviour between those for $\Delta_q = 50$ MeV and $\Delta_q = 0$. Heat transport becomes not efficient after first $5 \div 10$ yr. The subsequent 10^4 yr evolution is governed by QDU processes and quark specific heat being only moderately suppressed by the gaps and by the rates of NPBF processes in the hadronic matter (up to $\lg(t[\text{yr}]) \leq 2.5$). At $\lg(t[\text{yr}]) \geq 4$ begins the photon cooling era.

The curves for normal quark matter ($\Delta_q = 0$) are governed by the heat transport at times $t \lesssim 5$ yr and then by QDU processes and the quark specific heat. The NPBF

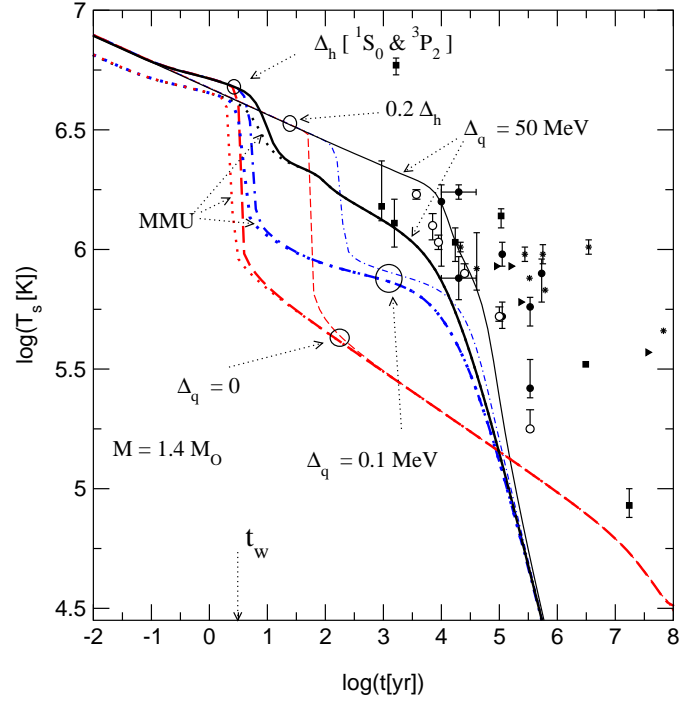


Fig. 2. Evolution of the surface temperature T_s of HNS with $M = 1.4M_\odot$ for $T_s \propto T_m^{2/3}$. Data points are from Schaab et al. (1999) (full symbols) and from Yakovlev et al. (2000) (empty symbols). t_w is the typical time which is necessary for the cooling wave to pass through the crust.

processes are important up to $\lg(t[\text{yr}]) \leq 2$, the photon era is delayed up to $\lg(t[\text{yr}]) \geq 7$. For times smaller than t_w (see Fig. 2) the heat transport is delayed within the crust area (Lattimer et al. 1991). Since we, for simplicity, disregarded this delay in our heat transport treatment, for such small times the curves should be interpreted as the $T_m(t)$ dependence scaled to guide the eye by the same law $\propto T_m^{2/3}$, as T_s .

5. Temperature evolution of QCNS

5.1. Temperature profiles $T(r, t)$

As can be seen from the lower panel of Fig. 3 for our large gap example ($\Delta_q = 50$ MeV), where $Y_e \neq 0$ is determined from equation of state, the QCNS cools down rather smoothly from its surface during the first 300 yr.

All the small gap examples exhibit about the same behaviour as the case $\Delta_q = 0.1$ MeV which we present in the upper panel of Fig. 3. Opposite to the large gap case, the transport processes are very efficient and a homogeneous temperature profile is recovered at $t \ll 10^{-5}$ yr. In reality in the latter case $T(r_m, t) \simeq T(r_m, 0)$ at times $\ll 1$ yr with a drop of $T(r)$ in a narrow interval near $r/r_m = 1$ and we disregard this peculiar behaviour as we have explained this above discussing HNS.

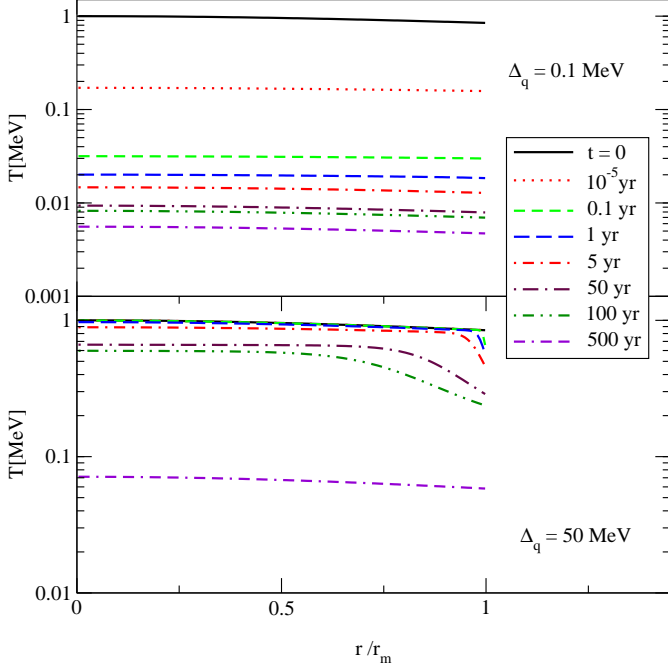


Fig. 3. Early evolution of temperature profiles for a QCNS of $M = 1.4M_{\odot}$ with large (lower panel), and small (upper panel) diquark pairing gaps.

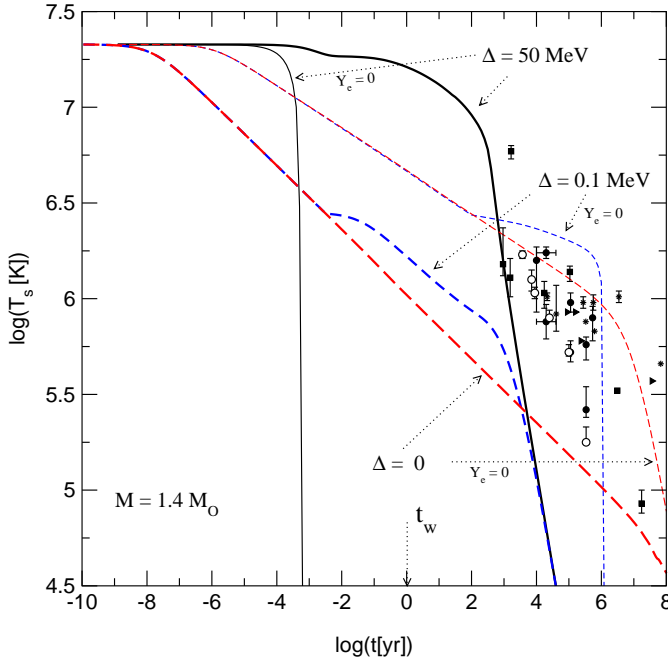


Fig. 4. Evolution of the surface temperature T_s for the QCNS with $M = 1.4M_{\odot}$ for $T_s \propto T_m^{2/3}$.

5.2. Evolution of the surface temperature

In Fig.4 we demonstrate the evolution of the surface temperature $\lg T_s$ vs. $\lg t$ for representative cases. The curve for $\Delta_q = 50$ MeV ($Y_e \neq 0$) shows a 300 yr delayed cooling which then is controlled by the electron specific heat and

the photon emissivity from the surface, as it was stated in (Blaschke et al. 2000). However, in difference with the corresponding curve of (Blaschke et al. 2000) we have a much larger typical cooling time scale ($t \sim 300$ yr) since in that work the simplifying approximation of a homogeneous temperature profile has been used. For the low gap limit $\Delta_q \ll 10$ MeV in this particular QCNS case there is no heat transport delay and our results coincide with those obtained in (Blaschke et al. 2000). Unimportant differences are only due to the inhomogeneous density profile and a different value of $Y_e(n)$ which follows in our case from an actual calculation for the given equation of state. The curve corresponding to $\Delta_q = 0.1$ MeV ($Y_e \neq 0$) from very early times is due to a competition between QDU emissivity and the quark specific heat, both being only moderately suppressed whereas late time asymptotics, as in the large gap example, relates to the photon era. A similar trend is present for normal quark matter staying below the corresponding curves for $\Delta_q = 0.1$ MeV due to the absence of the ζ suppression factors in the former case. At $t > 10^8$ yr both cases have a different photon era asymptotic behaviour whereas all finite gap curves have the same large time asymptotics when $Y_e \neq 0$.

At $Y_e = 0$ the QDU processes are absent and the large time asymptotics are governed by the gluon-photon specific heat which is a nonlinear function of the temperature and the photon emissivity. Due to this nonlinearity the large time asymptotics are different in all the cases under consideration. All the results for $Y_e = 0$ (including case of large gaps) coincide with those obtained in (Blaschke et al. 2000) although the sharp fall of the curve for the large gap case is in reality controlled by the heat conductivity of the crust that will lead to a cooling delay within the first year of evolution (Pizzochero 1991) as in Fig. 2 the curves for $t < t_w$ should be interpreted as $T_m(t)$ dependence scaled by the Tsuruta law.

6. Conclusion

For the CFL phase with large quark gap, which was expected to exhibit the most prominent manifestations of colour superconductivity in HNS and QCNS, we have found an essential delay of the cooling during the first $50 \div 300$ yr due to a dramatic suppression of the heat conductivity in the quark matter region. This delay makes the cooling of QCNS not as rapid as one could expect when ignoring the heat transport. In HNS compared to QCNS (large gaps) an additional delay of the subsequent cooling evolution comes from the processes in pure hadronic matter. In spite of that we found still too fast cooling for those objects. Therefore, with the CFL phase of large quark gap it seems rather difficult to explain the majority of the presently known data both in the cases of the HNS and QCNS, whereas in the case of pure hadronic stars the available data are much better fitted within the same model for the hadronic matter we used here. For 2SC (3SC) phases we expect analogous behaviour to that demonstrated by $\Delta_q = 0$ since QDU processes on unpaired

quarks are then allowed. We however do not exclude that new observations may lead to lower surface temperatures for some supernova remnants and will be better consistent with the model which also needs further improvements. On the other hand, if future observations will show very large temperatures for young compact stars they could be interpreted as a manifestation of large gap color superconductivity in the interiors of these objects.

Acknowledgements. Research of H.G. and D.B. was supported in part by the Volkswagen Stiftung under grant no. I/71 226 and by DFG under grant no. 436 ARM 17/1/00. H.G. acknowledges the hospitality of the Department of Physics at the University of Rostock where this research has been performed. D.N.V. is grateful for hospitality and support of GSI Darmstadt. D.B. acknowledges support of the Department of Energy for his participation in the INT program on “QCD at Nonzero Baryon Density” (INT-00-1) at the University of Washington as well as a fellowship at the ECT* Trento where this work was completed. We thank Th. Klähn for his contributions during early stages of this work; M. Colpi, M. Prakash, K. Rajagopal, S. Reddy, A. Sedrakian and F. Weber for their discussions during the Workshop “Physics of Neutron Star Interiors” at the ECT*.

References

- Alford, M., Rajagopal, K., Wilczek, F., 1998, Phys. Lett. B 422, 247
- Baiko, D. A., Haensel, P., 1999, Acta Phys. Polon. B 30, 1097
- Blaschke, D., Klähn, T., Voskresensky, D.N., 2000, ApJ 533, 406
- Carter, G.W., Reddy, S., 2000, Phys. Rev. D 62, 103002.
- Chubarian, E., Grigorian, H., Poghosyan, G., Blaschke, D., 2000, A&A. 357, 968
- Duncan, R.C., Shapiro, S.L., Wasserman, I., 1983, ApJ 267, 358
- Flowers, E., Itoh, N., 1981, ApJ 250, 750
- Flowers, E., Ruderman, M., Sutherland, P., 1976, ApJ 205, 541
- Friman, B., Maxwell, O., 1979, ApJ 232, 541
- Glendenning, N.K., 1996, *Compact Stars*, New York: Springer
- Gudmundsson, E.H., Pethick, C.J., Epstein, R.I., 1982, ApJ 259, L19
- Gudmundsson, E.H., Pethick, C.J., Epstein, R.I., 1982, ApJ 272, 286
- Haensel, P., Jerezak, A.J., 1989, Acta Phys. Pol. B 20, 141
- Iwamoto, N., 1982, Ann. Phys. 141, 1
- Kaminker, A.D., Haensel, P., 1999, Acta Phys. Pol. B 30, 1125
- Lattimer, J.M., Pethick, C., Prakash, M., Haensel, P., 1991, Phys. Rev. Lett. 66, 2701
- Maxwell, O. V., 1979, ApJ 231, 201
- Migdal, A. B., Saperstein, E. E., Troitsky, M. A., Voskresensky, D. N., 1990, Phys. Rep. 192, 179
- Page, D., 1992, *High Energy Phenomenology*, M. A. Perez and R. Huerta, Singapore: World Scientific, p. 347
- Page, D., M. Prakash, J. M. Lattimer, A. Steiner, 2000, Phys. Rev. Lett. 85, 2048
- Potekhin, A.Y., Chabrier, G., Yakovlev, D.G., 1997, A & A 323, 415
- Pizzochero, P.M., 1991, Phys. Rev. Lett. 66, 2425
- Rapp, R., Schäfer, T., Shuryak, E.V., Velkovsky, M., 1998, Phys. Rev. Lett. 81, 53
- Rapp, R., Schäfer, T., Shuryak, E.V., Velkovsky, M., 2000, Ann. Phys. 280, 35
- Reddy S., Bertsch G., Prakash M., 2000, Phys. Lett. B 475, 1
- Schaab, Ch., Voskresensky, D., Sedrakian, A.D., Weber, F., Weigel, M.K., 1997, A & A 321, 591
- Schaab, Ch., Sedrakian, A., Weber, F., Weigel, M.K., 1999, A & A 346, 465.
- Shapiro, S., Teukolsky, S.A., 1983, *Black Holes, White Dwarfs and Neutron Stars*, New York: Wiley, ch. 10.
- Tsuruta, S., 1979, Phys. Rep. 56, 237
- Van Riper, K.A., 1988, ApJ 329 339
- Voskresensky, D. N., Senatorov, A. V., 1987, Sov. J. Nucl. Phys. 45, 411
- Voskresensky, D. N., Senatorov, A. V. 1986, JETP 63, 885
- Weber, F., 1999, *Pulsars as Astrophysical Laboratories for Nuclear and Particle Physics*, Bristol: IoP Publishing
- Yakovlev, D. G., Levenfish, K. P., Shibano, Yu. A., 1999, Phys. Usp. 42, 737